Flapping Membrane Wing: A Prediction towards Inter-Domain Flight

Abas, M. F.[1], Aftab, S. M. A.[1], Rafie, A. S. M.[1], Yusoff, H.[2] and Ahmad, K. A.[1]*

[1]*Department of Aerospace Engineering, Faculty of Engineering, Universiti Putra Malaysia, 43400 UPM Serdang, Selangor, Malaysia*

[2]*Faculty of Mechanical Engineering, Universiti Teknologi MARA Pulau Pinang, 13500 Permatang Pauh, Pulau Pinang, Malaysia*

ABSTRACT

The purpose of this research is to gain initial knowledge and to predict the sustainability of an all-weather Micro-Aerial-Vehicle (MAV). The observed parameters are: the maximum coefficient of lift, C_L and the changes in C_L after impact, the fluctuation of C_L upon entering simulated rain environment, and length of stability recovery in terms of time and flapping cycle, t and t/T, at flapping frequencies of 8, 16, and 24 Hz, at t/T = 3/8 and 7/8. At 24 Hz, the increase in peak C_L value after impact of entering rain environment is 0.59. The average fluctuations in C_L occurred when entering the rain environment are 410.263. The stability recovery time recorded is 0.006 seconds. Small birds (especially hummingbirds) have a very high flapping frequency that enables them to efficiently withstand external disturbances caused by nature and to instantly adapt to new environments.

Keywords: Membrane wing, flapping, flat plate, inter-domain, flapping stability, simulated rain

INTRODUCTION

The DARPA (The Defense Advanced Research Projects Agency) defines Micro-Aerial-Vehicle (MAV)as an aerial vehicle that has; a maximum wingspan of 15cm. Producing a small size flapping vehicle inspired by biomimetics of birds has been a very challenging feat, even more when designing a flapping vehicle that has a size of an insect. There are a lot of factors and variables to consider, and a lot more to be discovered. As MAV has a very short wingspan, lift and thrust production are limited to the ability of the MAV's wings to manipulate airflow in its surroundings to counter any shortcomings.

External disturbance is also a potential factor in determining the reliability of a certain MAV, with larger concerns when attempting to achieve and produce an all-weather MAV (a MAV that could be operated under any weather condition).

One of the simplest ways to produce enough lift and thrust force for a very short wingspan is to reduce its aspect ratio (AR). Tsai and Fu (2005) have proven that a wing with AR of 3 can produce lift equivalent to a wing with AR of 8 given the right chord length and flight speed. Referring to the external disturbance factor, Warrick et al . (2005) discovered that hummingbird wing motion exhibits a figure-eight pattern and is highly adaptive to accommodate the challenges posed by wind gust. To top it off, AeroVironment (http://www.avinc.com/) uses a hummingbird-like flapping wing design that can withstand a 2 m/s wind gust from the side without drifting more than 1m.

On the other hand, Lee et al. (2011) discovered that longitudinal flight dynamics of a bio-inspired ornithopter with a reduced-order aerodynamics model and wing flexibility effects showed robustness towards external disturbances due to its trimmed flight dynamic characteristics. Niu et al. (2012), Lee et al. (2008), and Kim et al. (2005) conducted a preliminary study of three-dimensional aerodynamics, experimental evaluation of aerodynamic model, and a comparative study of rigid and flexible wing in flapping motion respectively. Combes and Dudley (2009) have discovered that bees have the ability to overcome external disturbances as well by means of wing-body interactions to regain aerodynamic stability. Lian et al. (2003) reported that the advantage of a flexible membrane wing is that it can adapt to wind gust and provide a smoother flight platform, which has been proven experimentally by Shyy et al. (1997). Furthermore, Shyy et al. (2013) have compiled all of his researches with a special subtopic addressing the effects of wind gust on hovering aerodynamics.

Limited research has been done on the other effects of external disturbances on flapping wing aerodynamics, such as rain, snow, and sandstorm due to the high complexity and difficulty of mimicking those environments and the vast amount of variables and unknowns to consider. The purpose of this research is to gain initial knowledge and to predict the sustainability of an all-weather MAV. In this research, a flat wing is simulated to flap through two different domains, from actual atmospheric air plunging through simulated "rainy" environment. An initial prediction on the effects of rain on flapping wing aerodynamic forces will be simulated by applying an assumption - rain environment is treated as modified water vapour environment with mixture density, ρ_{mix} and viscosity, μ_{mix}. The maximum coefficient of lift, C_L and the changes in C_L after impact, the fluctuation of C_L upon entering simulated rain environment, and length of stability recovery in terms of time and flapping cycle, t and t/T, will be observed for 8, 16, and 24 Hz flapping frequencies, f. The nomenclature associated in this research is shown in Table 1.

Table 1
Nomenclature

Symbol	Quantity	SI Units
$y(t)$	wing motion with respect to time	m
h_a	flapping amplitude	m
Fh	flapping oscillating frequency	Hz
T	time	s
φ_h	phase angle	°

[a]SI Units: s = seconds, m = meter, Hz = Hertz, ° = Degree angle

METHODOLOGY

Simulation Model

In this research, a rectangular flat plate wing has been considered for simplicity. The chord length of the wing, c is 5cm, the half wingspan length is 7.5cm, and the thickness is 0.03cm. The domain of the simulation is created using three-dimensional "C-mesh". The dimensions are 32.5c in length, 12.5c in width, and 25c in height. Two test domains were created, one with structured mesh "casing" to capture the boundary layer effects and increase the accuracy of the simulation as shown in Fig. 1a, and the other one without the structured mesh casing as shown in Fig. 1b. Both test domains have similar cell count; 633862 and 642544, with the former being the test domain with the structured mesh casing. The structured mesh casing has been set to move with the flapping motion of the membrane wing.
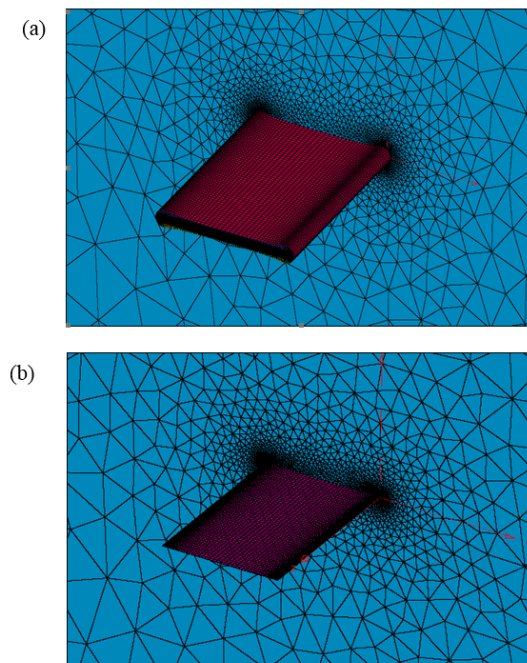

Figure 1. Membrane wing with structured mesh casing (a) and without structured mesh casing (b).

As shown in Figure 2, the movement of the structured mesh casing does not interfere with the pressure distribution on the wing and it has been observed that this domain produces faster simulation results compared with the one without the structured mesh casing by approximately one hour. The mesh was done using Pointwise V17.3R1 (2015) while simulation of the test domains were done using Ansys Fluent 15.0 (2013).
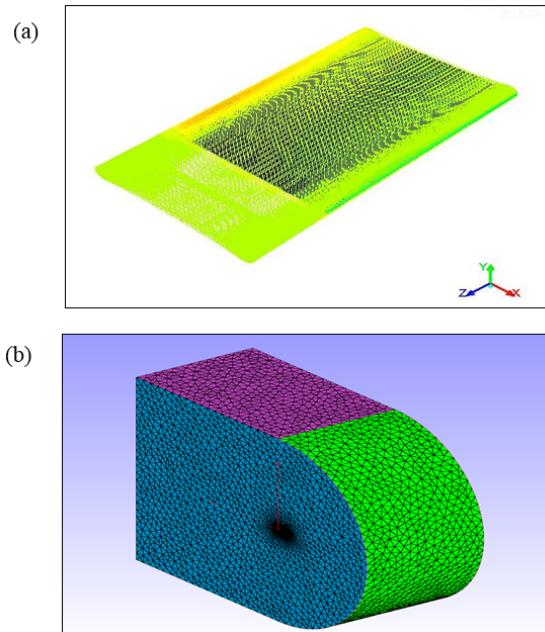
(a)

(b)

Figure 2. High pressure value at leading edge of membrane wing (a) and the 3D simulation domain (b).

The simulation was been done under unsteady (transient) conditions, utilising SIMPLE pressure-velocity coupling scheme, with pressure and momentum solver set to 2nd order upwind under spatial discretisation criteria. A simple harmonic function (pure flapping) was adopted for the membrane wing flapping motion.

$$y(t) = h_\alpha cos(2\pi f_h t + \varphi_h)$$

where h_α is the flapping amplitude (30˚) and is defined positive upwards, $2\pi f_h$ is the flapping angular frequency, f_h is the flapping oscillating frequency (8, 16, 24 Hz), and φ_h is the phase angle of the flapping motion (15˚). The flapping flight velocity was set to 10 m/s. The impact of rain environment will be initiated at two different instances, t/T = 3/8 and t/T = 7/8 as shown in Figure 3.
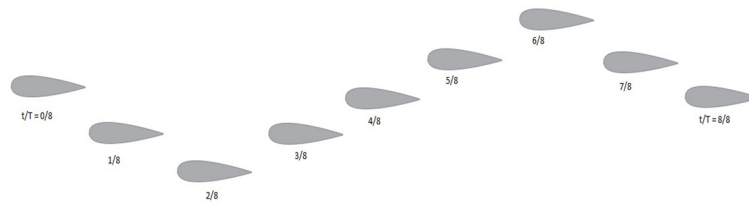
Figure 3. Visualisation of wingtip position viewed at normal of wingtip surface.

Validation of Model

The simulation of the flapping membrane wing in this research was validated using Tsai and Fu (2015) and Shi-Ming Huang (2004). Figure 4 below shows the comparison of the validation test case of the flapping membrane wing at 24 Hz flapping frequency. All calculations and comparisons are done with respect to the second flapping cycle to ensure optimum data accuracy.
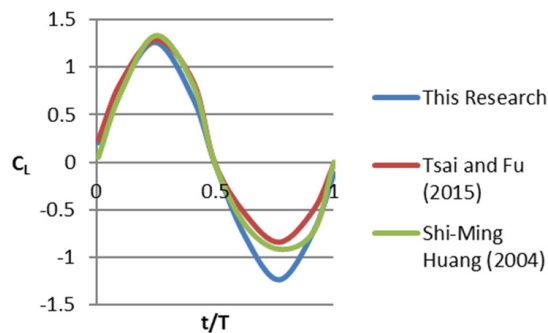

Figure 4. Validation case of flapping membrane wing at 24 Hz; this research, Tsai and Fu (2015), and Shi-Ming Huang (2004).

Rain Condition Prediction

To mimic a rainy environment, an assumption was made; rain particles were treated as modified water vapour particles with mixture density, ρ_{mix} and viscosity, μ_{mix}, since no published method or equation is currently available dedicated solely on calculating the actual density and viscosity of rainy atmosphere. Therefore, the following equations, as proposed by Davidson (1993) and Brokaw (1968), will be used to predict the density and viscosity of dry air-water vapour mixture:

$$D = \left(\frac{P}{Rd * T}\right)\left(1 - \frac{0.378 * Pv}{P}\right)$$

where
D = Density
P = Pd + Pv = Total air pressure
Pd = Pressure of dry air
Pv = Pressure of water vapour

$7Rd$ = Gas constant for dry air = 287.05 J/kg˚K
$7T$ = Temperature = 288.15 ˚K

Pressure of water vapour, Pv can be obtained using the following equation:

$$Es = c0\left(10^{\frac{c1*Tc}{c2+Tc}}\right)$$

where
As = Saturation pressure of water vapour
Tc = Temperature in ˚C
c0 = 6.1078
c1 = 7.5000
c2 = 237.3000

To predict the viscosity of dry air-water vapour mixture, the following equation was adopted:

$$\mu_{mix} = x_{dry\ air}\mu_{dry\ air} + x_{water\ vapor}w_{ave\ vapour}$$

where

μ_{mix} = viscosity of dry air-water vapour mixture

$x_{dry\ air}$ = mole fraction of dry air

$x_{water\ vapour}$ = mole fraction of water vapour

$\mu_{dry\ air}$ = viscosity of dry air

$\mu_{water\ vapour}$ = viscosity of water vapour

Using all the equations above, the value of dry air-water vapour mixture's density, ρ_{mix} will be set to 1.2378 kgm^{-3} and the value of dry air-water vapour mixture's viscosity, μ_{mix} will be set to 1.597x10^{-5} *kgm-1s-1*.

RESULTS AND DISCUSSION

Maximum coefficient of lift, C_L before and after impact

In this research, the maximum achievable coefficient (peak value) of lift, C_L during upstroke and downstroke was observed for membrane wing with flapping frequency of 8 Hz, 16 Hz, and 24 Hz, before and after the impact of crossing from atmospheric air into the simulated rain environment. The peak CL for all three of the flapping wing frequencies is as shown in Figure 5.

For flapping frequency of 8 Hz, the peak C_L value stabilises at an average value of ±0.405 and for flapping frequency of 16 Hz, the peak C_L value stabilises at an average value of ±0.891. Meanwhile for flapping frequency of 24 Hz, the peak C_L value stabilises at an average value of ±1.266. These peak C_L values achieved stability after the second flapping cycle within the air domain before entering the simulated rain domain. As mentioned in the methodology section above, peak C_L values are taken from the second flapping cycle to ensure optimum accuracy. These stabilised peak C_L values agree with the simulation results produced by Tsai and Fu (2015) and Shi-Ming Huang (2004).

After entering the rain environment and immediately after the peak C_L values regained stability, a slight increase in peak C_L values for all three flapping frequencies was observed.

At t/T = 3/8 impact position, an increase of peak C_L values of approximately 0.21, 0.53, and 0.56 were observed at 8, 16, and 24 Hz respectively. Meanwhile at t/T = 7/8 impact position, a slightly larger increase in peak C_L values were recorded as compared to the increase in peak C_L values at t/T = 3/8, which yielded an increase of peak C_L values of approximately 0.23, 0.57, and 0.62 at 8, 16, and 24 Hz respectively.
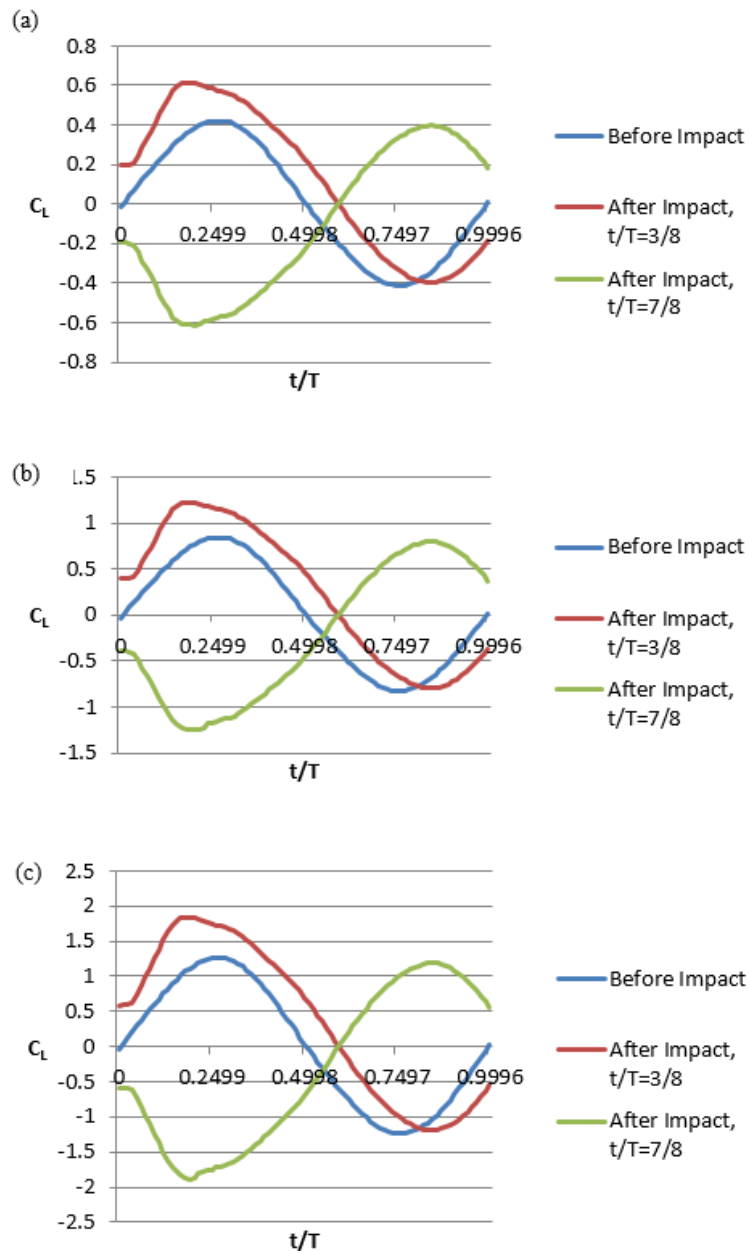

Figure 5. Peak C_L before and after impact of rain environment; 8 Hz (a), 16 Hz (b), 24 Hz (c)

Impact of rain domain

The effects of rain domain are applied at the $t/T = 3/8$ and $t/T = 7/8$ positions. Figure 6 a-c shows the fluctuations of C_L that occur upon impact at the boundary between air domain and rain domain. The maximum fluctuations of C_L are recorded for flapping frequency on 8, 16 and 24 Hz.

At $t/T = 3/8$, C_L fluctuation that occurred at flapping frequency of 8 Hz reached up to 140.505, which is more than 346 times the maximum value of stabilised C_L. For flapping frequency of 16 Hz, C_L fluctuated up to 261.031 and flapping frequency of 24 Hz recorded C_L fluctuation up to 409.522, which was more than 292 and 323 times the maximum value of stabilised C_L for 16 Hz and 24 Hz respectively.

At $t/T = 7/8$, it can be observed that the maximum value of C_L fluctuations is similar to its $t/T = 3/8$ position counterpart. Flapping frequency of 8 Hz recorded a maximum value of C_L fluctuation of up to -140.997 ("-" sign indicates downstroke direction). Meanwhile flapping frequencies of 16 Hz and 24 Hz recorded a maximum value of C_L fluctuation of up to -260.374 and -411.003 respectively. Therefore, we can safely assume that the values C_L fluctuation at $t/T = 7/8$ are the same in magnitude with $t/T = 3/8$ (less than 10 percent difference) but in different direction (caused by upstroke and downstroke motions).

It is observed that fluctuations occurred more than a 100 folds more than the recorded stabilised C_L. With this much amplification of peak C_L, aerodynamic instability will definitely occur during the flapping flight. The fluctuation of peak C_L only happens within a narrow time frame of 0.0035 to 0.0195 seconds. Within that short window of opportunity, a flapping wing MAV must be able to adapt and regain aerodynamic stability in order to maintain air superiority.

Stability Recovery

As mentioned in the previous section, a flapping wing MAV needs to be able to adapt towards any form of peak C_L fluctuations within an instance to maintain aerodynamic stability. It is important for us to understand and estimate the period of time a flapping wing MAV takes to regain stability of its flapping wing peak C_L value in order to produce a sustainable all-weather MAV. As shown in Figure 7a-b, the length of stability recovery in terms of time and flapping cycle, t and t/T, are observed for 8, 16, and 24 Hz flapping frequencies at $t/T = 3/8$ and $t/T = 7/8$ impact positions.

At impact position $t/T = 3/8$, a flapping membrane wing that flaps at 8 Hz recovers its stabilised peak C_L value in 0.016 seconds, which is equivalent to 1.375 flapping cycle where as a flapping wing that flaps at 16 Hz recovers its stabilised peak C_L value in 0.011 seconds, which is equivalent to 1.4375 flapping cycle. Flapping at 24 Hz, a flapping membrane wing recovers its stabilised peak C_L value in 0.006 seconds, which is equivalent to 1.625 flapping cycle.

At impact position $t/T = 7/8$, the time and flapping cycle taken by a flapping membrane wing that flaps at 8 Hz, 16 Hz, and 24 Hz to recover stabilised peak C_L values are equivalent to its counterpart at impact position $t/T = 3/8$. With this results, we can conclude that a flapping wing MAV that flaps at 24 Hz is able to adapt to the impact of entering the simulated rain environment the fastest with only 0.006 seconds of recovery time.
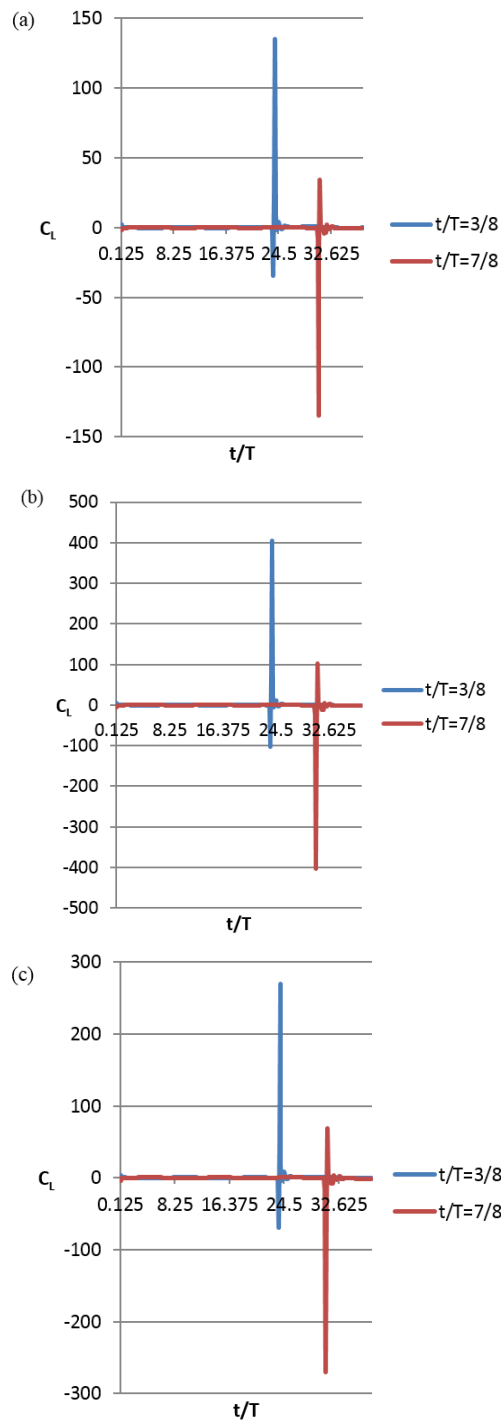
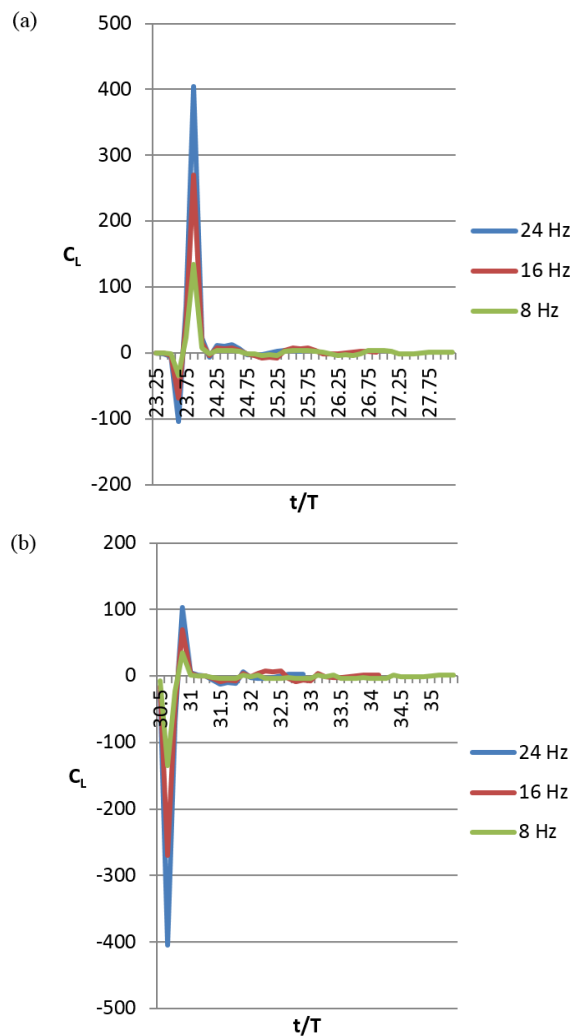*Figure 6*. Fluctuation at 8 Hz (a), 16 Hz (b), and 24 Hz (c)

Figure 7. Stability recovery period at t/T = 3/8 (a) and t/T = 7/8 (b) at 8 Hz, 16 Hz, and 24 Hz

CONCLUSION

In this research, a flapping membrane wing has undergone impact of inter-domain flight from atmospheric air into a simulated rain environment at an impact position of t/T = 3/8 and 7/8. Three flapping frequencies, 8 Hz, 16 Hz, and 24 Hz have been considered for this research. As a conclusion, at 8 Hz flapping frequency, the increase in peak C_L value after impact of entering rain environment is the lowest among the three flapping frequencies, which is only by an average of 0.22. The fluctuations that occurred are also the lowest among the three flapping frequencies, up to an average of 140.751. At 8 Hz flapping frequency, the stability recovery time recorded is 0.016 seconds, which is the longest stability recovery time among the three flapping frequencies.

At 24 Hz flapping frequency, the increase in peak C_L value after impact of entering rain environment is the highest, which is by an average of 0.59. The fluctuations that occurred are also the highest, up to an average of 410.263. At 24 Hz flapping frequency, the stability recovery time recorded was 0.006 seconds, which is the shortest stability recovery time among the three flapping frequencies. The results of this research can very well explain as to why small birds (especially hummingbirds) have a very high flapping frequency. It is to enable them to efficiently withstand external disturbances caused by nature and to instantly adapt to new environments.

REFERENCES

Brokaw, R. S. (1968). *Viscosity of Gas Mixtures* (Report No. NASA TN D-4496). Washington D. C.: National Aeronautics and Space Administration.

Combes, S. A., & Dudley, R. (2009). Turbulence-driven instabilities limit insect flight performance. *Proceedings of the National Academy of Sciences, 106*(22), 9105-9108..

Davidson, T. A. (1993). *A Simple and Accurate Method for Calculating Viscosity of Gaseous Mixtures* (Report No. RI9456). USA: Bureau of Mines.

Huang, S. M. (2004). *Numerical simulation of flow over a flapping wing* (Doctoral dissertation). National Cheng Kung University, Tainan City, Taiwan.

Kim, Y. J., Choi, H. C., & Kim, K. H. (2005). The comparative study of rigid wing and flexible wing in flapping motion. *AIAA Atmospheric Flight Mechanics Conference and Exhibit*, Paper No. 2005-6336.

Lee, J. S., Kim, D. K., Lee, J. Y., & Han, J. H. (2008). Experimental evaluation of a flapping-wing aerodynamic model for MAV applications. *SPIE 15th Annual Symposium Smart Structures and Materials*, *6928*(69282M), 1-8.

Lee, J. S., Kim, J. K., Kim, D. K., & Han, J. H. (2011). Longitudinal flight dynamics of bioinspired ornithopter considering fluid-structure interaction. *Journal of Guidance, Control, and Dynamics*, *34*(3), 667-677.

Lian, Y., Shyy, E., Viieru, D., & Zhang, B. (2003). Membrane wing aerodynamics for micro air vehicles. *Progress in Aerospace Sciences*, *39*(6), 425-465.

Niu, Y. Y., Liu, S. H., Chang, C. C., & Tseng, T. I. (2012). A preliminary study of the three-dimensional aerodynamics of flapping wings. *Journal of Applied Science and Engineering*, *15*(3), 257-263.

Shyy, W., Aono, H., Kang, C. K., & Liu, H. (2013). *An Introduction to Flapping Wing Aerodynamics*. New York, NY: Cambridge University Press.

Shyy, W., Jenkins, D. A., & Smith, R. W. (1997). Study of adaptive shape airfoils at low Reynolds number in oscillatory flow. *American Institute of Aeronautics and Astronautics Journal*, *35*(9), 1545-1548.

Tsai, B. J., Fu, Y. C. (2005). Design and aerodynamic analysis of a flapping-wing micro aerial vehicle. *Aerospace Science and Technology*, *13*(7), 383-392.

Warrick, D. R., Tobalske, B. W., & Powers, D. R. (2005). Aerodynamics of the hovering hummingbirds. *Nature, 435*(7045), 1094-1097.